

—Report—

A new method for estimating the area of the seafloor from oblique images taken by deep-sea submersible survey platforms

Ryota Nakajima^{1*}, Tetsuya Komuku², Takehisa Yamakita³, Dhugal J. Lindsay⁴, Yoshie Jintsu-Uchifune⁴, Hiromi Watanabe¹, Katsuhiko Tanaka⁵, Yoshihisa Shirayama⁶, Hiroyuki Yamamoto⁴, and Katsunori Fujikura¹

In order to extract quantitative information on deep-sea benthic animals (no. individuals or biomass in an area) using oblique video/photo images taken by deep-sea submersible survey platforms, a new method was established to estimate the imaged area of the seafloor from the oblique images. The trapezoidal area appearing on the lower half of the screen was calculated using underwater horizontal and vertical aperture angles of the camera, the angle of incidence of the camera, and the camera-to-seafloor distance. The incidence angle of the camera was obtained using the angles of vehicle pitch and camera tilt, while the camera-to-seafloor distance was calculated from the lens-to-vehicle bottom distance, horizontal distance of lens-to-altimeter, and vehicle altitude. The areas estimated by the present method from images taken by some submersible survey platforms were comparable to those that were actually measured. With the above parameters, and by focusing on the lower half of an image, our method can be used for estimating the seafloor area from any oblique video/photo images taken by any submersible survey platform. Thus, this method is useful for the extraction of quantitative data on benthic animals from legacy oblique video/photographs acquired by submersible survey platforms.

Keywords : area, benthos, oblique image, deep-sea, trapezoid

Received 1 April 2014 ; Revised 24 June 2014 ; Accepted 24 June 2014

- 1 Department of Marine Biodiversity Research, Japan Agency for Marine-Earth Science and Technology (JAMSTEC)
- 2 Nippon Marine Enterprises, Ltd (NME)
- 3 Habitat and ecosystem mapping unit, Tohoku Ecosystem-Associated Marine Sciences (TEAMS) project team, Japan Agency for Marine-Earth Science and Technology (JAMSTEC)
- 4 Submarine Resources Research Project, Japan Agency for Marine-Earth Science and Technology (JAMSTEC)
- 5 Department of Marine Biology, School of Marine Science and Technology, Tokai University
- 6 Japan Agency for Marine-Earth Science and Technology (JAMSTEC)

*Corresponding author:

Ryota Nakajima

Department of Marine Biodiversity Research, Japan Agency for Marine-Earth Science and Technology (JAMSTEC)

2-15 Natsushima-cho, Yokosuka, Kanagawa 237-0061, JAPAN

Tel.+81-46-867-9533

nakajimar@jamstec.go.jp

Copyright by Japan Agency for Marine-Earth Science and Technology

1. Introduction

Video and/or photo images taken by submersible survey platforms are helpful in understanding biological, geological and topographic settings in the deep-sea. In a biological study, these images are not just useful for obtaining qualitative information such as the distribution of deep-sea benthos, but also for obtaining quantitative information, such as abundance (e.g. individual m^{-2}) and biomass (e.g. $mg\ m^{-2}$) (e.g. Ohta and Laubier, 1987; Fujikura et al., 1995, 1996, 2002). To date, various deep-sea survey platforms with a variety of camera systems have been operated by JAMSTEC – dating back to the 1980s (Fujikura et al., 2008). Extraction of quantitative information on deep-sea benthic animals in various regions, using these the accumulated video/photo records, is necessary for understanding long-term changes and obtaining baselines to assess the impact of catastrophic events such as the 2011 Tōhoku earthquake (Seike et al., 2013) or the effects of deep-sea mineral mining (Collins et al., 2013).

Extraction of quantitative information (e.g. abundance or biomass) requires information on the area of the seafloor that was imaged (e.g. m^2). A down-facing camera mounted on a submersible, ROV or deep-towed camera system is often used to estimate the area of the seafloor (e.g. Fujikura et al., 1995, 2002; Jones et al., 2007; Guinan et al., 2009). The area (S) appearing in a downward-looking image can easily be estimated using the following equation (see Figs. 1a, b):

$$S = 4a^2 \tan(\alpha/2) \tan(\beta/2) \quad (1)$$

where a is the distance from the camera lens to the seafloor, and α and β are the vertical and horizontal aperture angles of the camera, respectively (Jones et al., 2007). However, most of the video/photo images taken by JAMSTEC's submersible survey platforms are from forward-facing cameras, angled obliquely towards the seafloor (Figs. 2a-d), and thus the above equation is not applicable.

In an image angled obliquely towards the seafloor (hereafter “oblique image”), the seafloor appears in the image in a trapezoidal geometry, with the imaged area expanding into the distance (i.e. the upper part of the image). In a previous study, Rice et al. (1979, 1982) obtained area values from oblique images for a quantitative study of deep-sea benthos, but their images were taken by camera

mounted on a bottom sledge, where camera-to-seafloor distance and camera tilt angle are fixed. Unlike the camera with the sledge, submersible survey platforms such as human occupied vehicles (HOVs) and remotely-operated vehicles (ROVs) face the problem that the angles of camera tilt and vehicle pitch vary significantly during transects, which leads to significant fluctuations in the imaged area of the seafloor. Previously, Chevaldonné and Jollivet (2003) estimated the imaged seafloor area from oblique images taken by deep-sea submersible survey platforms, but their equation can only be used for images where camera tilt is nearly vertical. In contrast, most images taken by JAMSTEC submersible platforms have a relatively wide field of view with a much shallower tilt angle of the cameras (Figs. 2b-d). In such cases, the depth of an image is often infinite, making it impossible to apply the method of Chevaldonné and Jollivet (2003). Moreover, the upper half of images is always dark – in most cases due to insufficient illumination, which makes it difficult to count, identify, and sometimes even to recognize the benthic animals. In this paper, we report a new method to estimate the imaged area of the seafloor from oblique images taken with a shallow camera tilt.

2. Methods

The present study estimated the area of only the lower half of each image (Fig. 3a), because the incident point of the camera lens (C in Figs. 3a, b), that determines the angle of incidence (θ in Fig. 3b), lies exactly in the middle of the image. The angle of incidence (θ) is a vital parameter to measure the area from oblique images, and focusing only on the lower half (1/2) of an image, below the middle point, makes the areal calculation easier than for the whole area or for other portions (e.g. 1/3, 3/4). The method also can be used on images with a much shallower tilt angle of the camera, where the depth of the upper part of the image is often infinite. The upper half of such images is often dark due to a lack of reflected light, and objects of interest within it are often too small to be identified reliably. Quantitative observations of only the lower half of each image enables identification and accurate counting of animals as they are much closer to the camera. (see Figs. 2a-d).

The necessary parameters for estimating the area of the lower half of the screen image (i.e. the trapezoidal area of $ABDE$ in Fig. 3b) were underwater vertical (α)

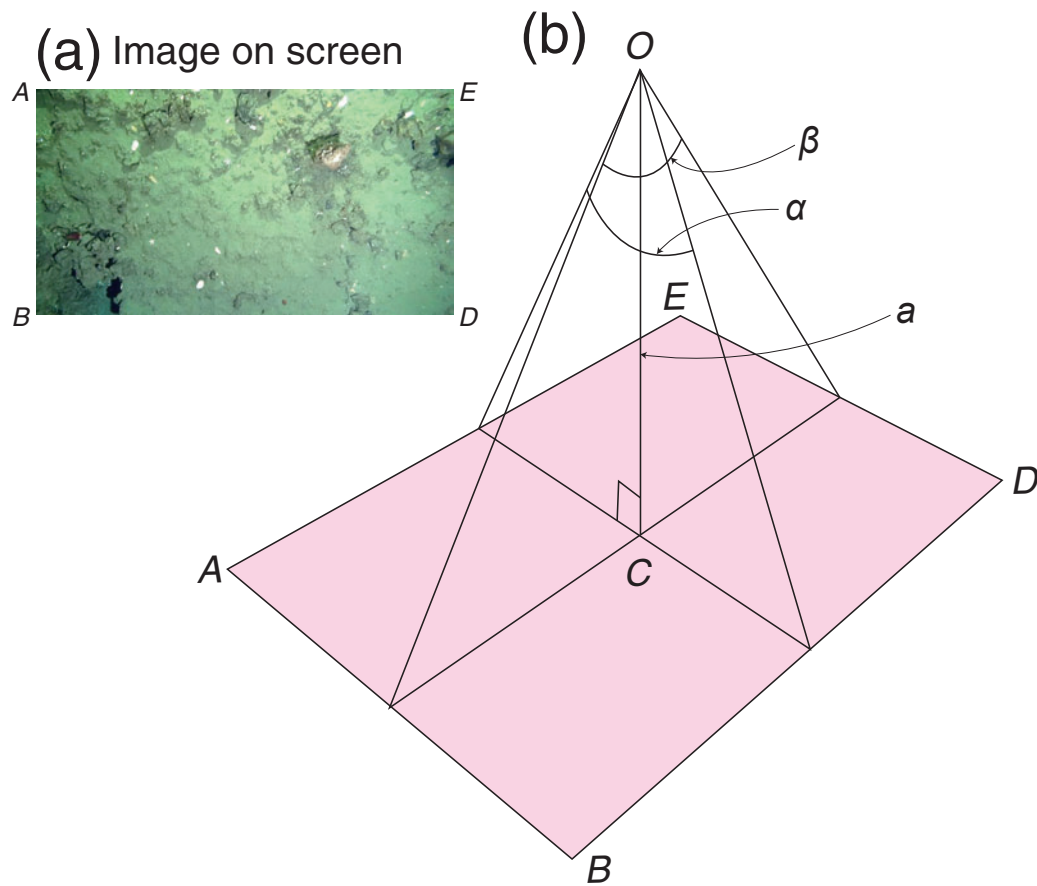


Fig. 1. An example of an image from a downward-looking camera (a) and a diagram of the sea-floor that appears in the image (b). O , origin (camera lens of submersible survey platform); C , image center; a , altitude (lens-to-image center distance); α , vertical aperture angle of the camera; and β , horizontal aperture angle of the camera.

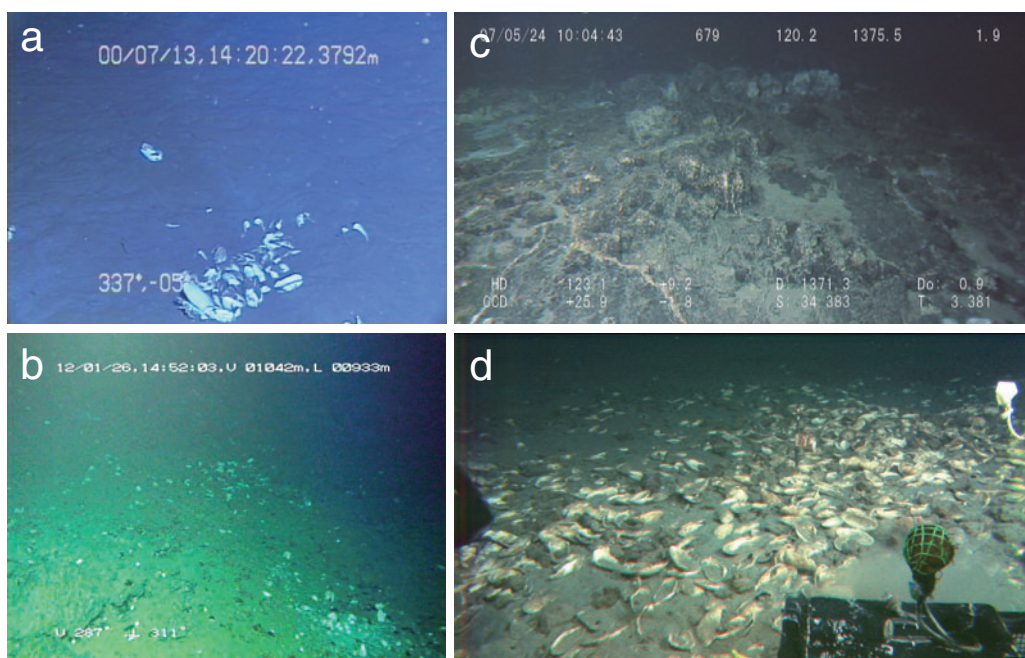


Fig. 2. Examples of oblique images taken by some submersible survey platforms. a, HOV *Shinkai 6500*; b, ROV *Kaiko 7000 II*; and c and d, ROV *Hyper-Dolphin*.

and horizontal (β) aperture angles of the camera, the angle of incidence of the camera (θ), and the camera-to-seafloor distance (OH). The incidence angle of the camera (θ) was obtained using the angles of vehicle pitch (η) and camera tilt (ρ), while the camera-to-seafloor distance (OH) was calculated from lens-to-vehicle bottom distance (a), horizontal distance of lens-to-altimeter (c), and vehicle altitude, as measured by an altitude meter (d). Among the necessary parameters, α , β , a , and c are vehicle-specific values and will vary depending on the submersible survey platform, while d , η and ρ are values of a variable. The d , η and ρ at intervals of a second or every few seconds are

generally logged and are available as text files post-dive.

The trapezoidal area (S) appearing on the lower half of the screen ($ABDE$ in Figs. 3a, b) was estimated as follows:

$$S(ABDE) = (AE + BD) \times CF / 2 \quad (2)$$

where AE and BD are the actual lengths of the lower and upper bases in the trapezoid $ABDE$, respectively, and CF is the vertical length of the trapezoid. AE , BD and CF were calculated as follows:

$$AE = 2 \tan(\beta/2)(OH \sin \theta^{-1}) \quad (3)$$

$$BD = 2 \tan(\beta/2)(OH \cos \delta^{-1}) \quad (4)$$

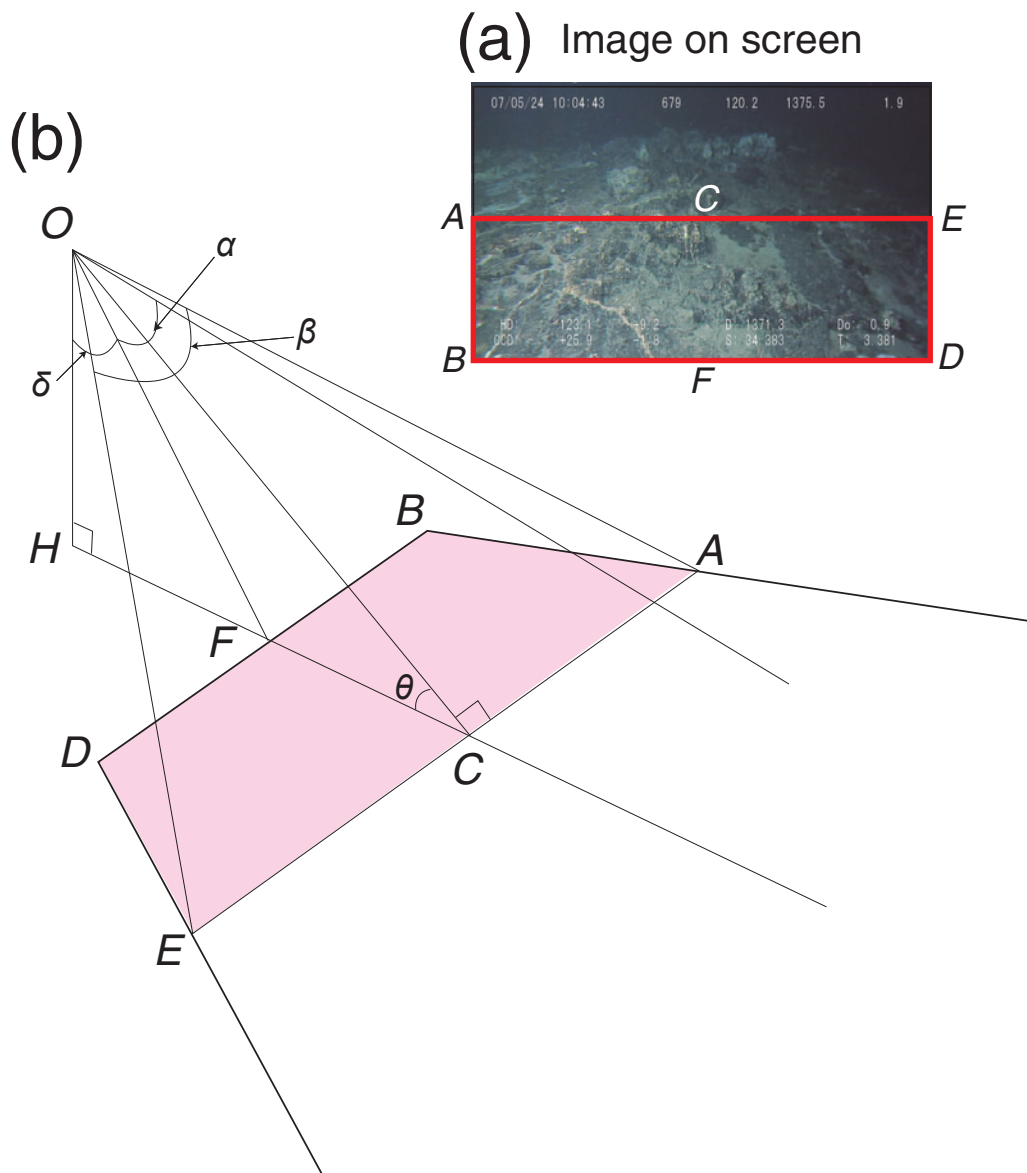


Fig. 3. An example of an oblique image, emphasizing the lower half of the image (a) and a diagram of the trapezoidal sea-floor that appears in the lower half of the image (b). O , origin (camera lens of submersible survey platform); C , image center; OC , lens-to-image center distance; OH , lens-to-seafloor distance; θ , angle of incidence; α , vertical aperture angle of the camera; and β , horizontal aperture angle of the camera.

$$CF = OH(\tan \theta^{-1} - \tan \delta) \quad (5)$$

where OH is the lens-to-seafloor distance, θ is the angle of incidence, and β is the horizontal aperture angle of the camera. δ was estimated as follows:

$$\delta = 180^\circ - (90^\circ + \theta + \alpha/2) \quad (6)$$

where α is the vertical aperture angle of the camera. θ was obtained by summing the angles of vehicle pitch (η) and camera tilt (ρ) (see Fig. 4):

$$\theta = \eta + \rho \quad (7)$$

where downward η angle is often expressed with a positive (+) value, while the downward ρ angle is often expressed with a negative (-) value. The lens-to-seafloor distance (OH) was obtained as follows:

$$OH = a \sin \gamma^{-1} - (a \tan \gamma^{-1} + c) \cos \gamma + d \sin(90^\circ - \eta) \quad (8)$$

where a is lens-to-vehicle bottom distance (see Fig. 4), c is horizontal distance of lens-to-altitude meter and d is altitude as measured by the altitude meter. γ was obtained as follows:

$$\gamma = 180^\circ - (90^\circ + \eta) \quad (9)$$

In order to test if our equations are reliable, we measured, with a tape measure, the exact area of the portion of the ship deck that was visible in the lower half of the field-of-view of the video camera of the HOV *Shinkai 6500* and ROV *Hyper-Dolphin*, and compared it with the value estimated using our equations. Since it was difficult to test in situ (i.e. above the seafloor), we compared the actual and estimated areas while the ROV (*Hyper-Dolphin*) was on deck during R/V Natsushima cruise (NT13-22) and while the crewed submersible *Shinkai 6500* was on land during its annual refitting. The focal length of the camera lens was adjusted to its minimum value (i.e. the field of view was at its maximum) during the experiment. Also the estimated area took into account the presence of a wide conversion lens, as

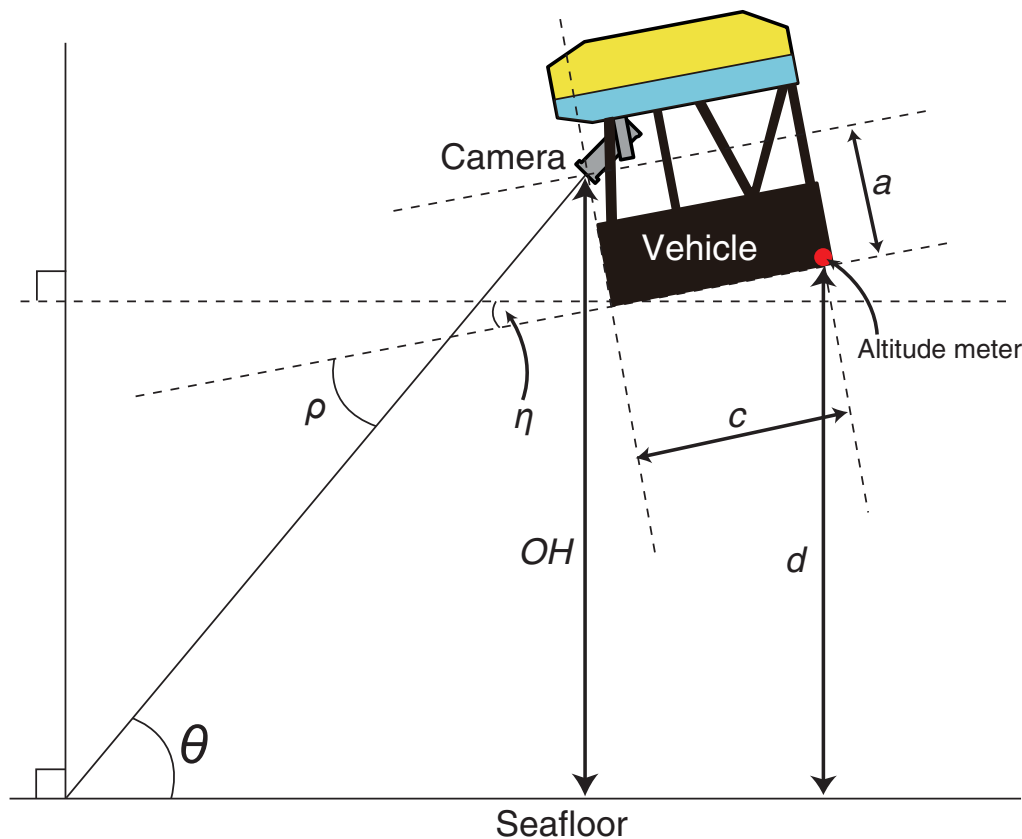


Fig. 4. Diagram of various angles and distances in relation to the vehicle camera. θ , angle of incidence; η , angle of vehicle pitch; ρ , angle of camera tilt; OH , camera lens-to-seafloor distance; a , lens-to-vehicle bottom distance; c , horizontal distance of lens-to-altitude meter; and d , altitude as measured by the altitude meter.

the ROV was equipped with a wide conversion lens ($\times 0.7$) at that time.

3. Results and Discussion

This report describes how to estimate the imaged area of the seafloor from oblique images taken by deep-sea submersible survey platforms. Obviously the use of a down-facing camera is more appropriate for quantitative studies, as it is simpler to calculate the seafloor area (Jones et al., 2007). However, most of the deep-sea images taken in the past by JAMSTEC submersible survey platforms are oblique images with sometimes-shallower camera tilt angles, and areas have to be estimated from these oblique images.

The estimated area of the lower half of an image taken by the *Shinkai 6500* (6.22 m^2) was almost equal to that actually measured (6.12 m^2). Similarly, the area estimated from an image taken by the *Hyper-Dolphin* (7.12 m^2) was comparable to that which was actually measured (6.94 m^2). Therefore, the method we have established can be used to estimate the imaged area of the seafloor from oblique images. In practice, a lens will always have a measure of distortion and thus β will have a range. However, most of the JAMSTEC submersible platforms use a wide-angle lens, which lowers the distortion. We therefore consider the error due to distortion to be negligible compared to the size of recognizable animals on the seafloor.

It should be noted that the ‘imaged area of the seafloor’ in our method is the projected area of a plain surface perpendicular to the gravity axis, and thus the method established in the present study is not strictly applicable over slopes. The estimated area would be overestimated with increasing inclination angle of the seafloor. Although the inclination angle of the seafloor for X- and Y-axes relative to the vehicle is difficult to measure, corrections will be required in some way if data on the angle of inclination is available. Similarly, our method assumes that the relative roll angle of the camera is near zero vs the seafloor. Therefore, the equations will not be applicable when the vehicle is rolling, even over flat seafloor perpendicular to the gravity axis. It should also be noted that our method is only applicable when the focal length of the camera is known, as it significantly affects the angles of vertical (α) and horizontal (β) aperture of the camera. Since the focal length of the camera is rarely recorded in

real-time during the course of the dive, it is important to analyze the oblique images with the minimum focal length of the camera. Although the method is somewhat limited due to these restrictions, still our method is useful for the extraction of quantitative data on benthic animals from legacy oblique video/photographs by submersible survey platforms, which would help our understanding of long-term changes in benthic animals, as well as for obtaining baseline data for environmental impact assessments.

We have summarized the specifications of cameras and lenses, including vertical (α) and horizontal (β) aperture angles, as well as the distances of lens-to-vehicle bottom (a) and lens-to-altitude meter (c), from various JAMSTEC submersible survey platforms (Table 1). These values are vehicle-specific and vary with respect to each submersible survey platform and date. The other information required is the output value of the altimeter (d) and the angles of vehicle pitch (η) and camera tilt (ρ), which are provided post-dive. With this information, our equations can be used for any oblique video/photo images taken by any submersible survey platform, including those from other institutions. However, some critical parameters, such as vehicle altitude and tilt angle of the cameras, and even latitude and longitude, are no longer available for some of the older JAMSTEC survey platforms (e.g. ROV *Dolphin 3K*, HOV *Shinkai 2000* and ROV *Kaiko*) as they have not been retained as records. Therefore the specifications of the cameras and lenses of these ‘old’ survey platforms are not included in Table 1.

The deep-sea video/photo images taken in the past by JAMSTEC submersible survey platforms are available from an image database (JAMSTEC E-library of Deep-sea Images, J-EDI) in the Global Oceanographic DATA Center (GODAC), where many of the images in which animals appear have been annotated (<http://www.godac.jamstec.go.jp/jedi/e/index.html>). With the information provided in Table 1 and data on the other parameters (i.e. altitude, vehicle pitch and camera tilt) for previous survey dives, the seafloor area of images and the abundances of animals (individuals m^{-2}) is also information that GODAC could conceivably provide in the future.

Acknowledgements

The authors thank Drs. T. Maruyama and Y. Furushima (JAMSTEC) who provided many helpful

Table 1. Summary of the specifications of cameras and lenses as well as the distances of lens-to-vehicle bottom and lens-to-altitude meter, used by various JAMSTEC deep-sea submersible survey platforms.

Deep-sea survey platform	Camera (angle)	Period (month/year)	Dive no.	Camera product name (manufacturer)	Image sensor (sensor size, inch)	Lens (manufacturer)	Focal length (mm)	Aperture angle of camera (tele°~wide°)		Vertical distance of camera lens-to-vehicle bottom (m)	Horizontal distance of camera lens-to-altitude meter (m)	
								horizontal (underwater)	vertical (underwater)			
<i>Shinkai 6500</i>	video1 (fixed, -37°to -40°)	4/1990-	1-	SP-3A (NEC) modified	CCD (2/3)	EJ10 mm (Canon) modified	10	46	35.9	1.7	2.8	
		5/2002-	671-	DXC-990 (Sony)	CCD (1/2)	S4×5.5BMD (Fujinon)	5.5~22	17.0~61.6	12.8~48.2	1.7	2.8	
		3/2010-	1177-	NC-H1000 (NEC)	CCD (2/3)	J12×10B4 (Canon) modified	10~120	4.6~52.2	2.6~29.3	1.7	2.8	
		3/2012-	1278-	NC-H1000 (NEC)	CCD (2/3)	ZA12×4.5BWMD (Fujinon)	4.5~54	~90	~57	1.7	2.8	
	video2 (pan-tilt)	4/1990-	1-	SP-3A (NEC) modified	CCD (2/3)	J12×10B4 (Canon) modified	10~120	4.2~47.5	3.2~36.5	1.7	2.65	
		8/2003-	772-	DXC-990 (Sony)	CCD (1/2)	S14×7.3BWMD (Fujinon)	7.3~110	3.6~47.3	2.7~36.4	1.7	2.65	
		3/2010-	1178-	FCB-H11 (Sony)	CMOS (1/3)	built-in	5.1~51	~ca.90 (ca.67)	~ca. 67.5 (ca.47.3)	1.7	2.65	
<i>Kaiko 7000</i>	TV1 (pan-tilt)	3/2004-	300-346	EVI-330 (Sony)	CCD(1/3)	built-in	5.4~64.8	4.3~48.3*	3.3~37.6*	1.25	2.47	
	TV2 (pan-tilt)	3/2004-	300-346	EVI-310 (Sony)	CCD (1/3)	built-in	5.9~47.2	5.8~44.3*	4.4~33.9*	1.25	2.47	
	TV3 (pan-tilt)	3/2004-12/2006	300-346	OE14-123 (Kongsberg)	CCD (1/4)	built-in	4.2~42	16.6~60.4*	12.5~47.1*	0.77	2.12	
<i>Kaiko 7000 II</i>	TV1 (pan-tilt)	4/2006-	347-	EVI-330 (Sony)	CCD(1/3)	built-in	5.4~64.8	4.3~48.3*	3.3~37.6*	1.6	2.75	
	TV2 (pan-tilt)	4/2006-	347-	EVI-310 (Sony)	CCD (1/3)	built-in	5.9~47.2	5.8~44.3*	4.4~33.9*	1.6	2.75	
	TV3 (pan-tilt)	4/2006-12/2006	347-376	OE14-123 (Kongsberg)	CCD (1/4)	built-in	4.2~42	16.6~60.4*	12.5~47.1*	0.97	2.75	
		4/2007-8/2012	377-555	TV3100XD (Photosea)	CCD (1/2)	?	5.4~38	9.6~61.3*	7.2~47.9*	0.97	2.75	
	HDV (fixed, angle?)	4/2006-	347-555	HVR-A1J (Sony)	CMOS (1/3)	Vario-Sonnar T (Carl Zeiss)	5.1~51	5.4~50.4*	4.0~38.9*	1.2	2.75	
	HDV (pan-tilt)	5/2010-8/2012	472-555	HDR-XR500V (Sony)	CMOS (1/2.88)	G lens (Sony)	5.5~66	4.3~48.9*	3.3~38.1*	0.97	2.75	
	HDTV1 (pan-tilt)	8/2012-	556-	FCB-H11 (Sony)	CMOS (1/3)	built-in	5.1~51	~ca.90** (ca.67)	~ca. 67.5** (ca.47.3)	0.97	2.75	
	HDTV2 (pan-tilt)	8/2012-	556-	FCB-H11 (Sony)	CMOS (1/3)	built-in	5.1~51	~ca.90** (ca.67)	~ca. 67.5** (ca.47.3)	0.97	2.75	
	<i>Hyper-Dolphin</i>	main video (pan-tilt)	8/2008-	1-1217	Super HARP (Hamamatsu Photonics)	Super HARP (2/3)	UW-S5×5.5-HD (?)	5.5~27.5	15.2~66.6*	8.9~41.7*	1.249	2.174
			12/2010-6/2011	1218-1283	FCB-H11 (Sony)	CMOS (1/3)	built-in	5.1~51	~ca.90** (ca.67)	~ca. 67.5** (ca.47.3)	0.869	1.598
6/2011-			1284-	FCB-H11 (Sony)	CMOS (1/3)	built-in	5.1~51	~ca.90** (ca.67)	~ca. 67.5** (ca.47.3)	1.249	1.756	
<i>PICASSO</i>	video 1 (main) (fixed, 0°)	2/2007-	1-	HDC-X300K (Sony)	CCD (1/2)	VCL-179BXS (Canon)	6.7~127	48.72	25.9	0.22	1.27	
	video 2 (stereo) (fixed, -7°)	2/2007-	1-	WAT-240 Vivid G-2.5 (Watec)	CCD (1/4)	built-in	3.8	80	59.3	0.35	1.24	
	video 3 (fixed, 0°)	2/2007-	1-	WAT-240 Vivid G-2.5 (Watec)	CCD (1/4)	built-in	3.8	80	59.3	0.69	-0.62	
	video 4 (fixed, -90°)	2/2007-	1-	WAT-240 Vivid G-2.5 (Watec)	CCD (1/4)	built-in	3.8	80	59.3	0.01	1.44	
<i>Crambon</i>	video (pan-tilt)	6/2013-	1-	FCB-H11 (Sony)	CMOS (1/3)	built-in	5.1~51	~ca.90** (ca.67)	~ca. 67.5** (ca.47.3)	0.328	1.294	
	still (fixed, -90°)	6/2013-	1-	FL3-GE-50S5C-C (Point Grey)	CCD (2/3)	LM8JC1MS (Kowa)	8	54.4 (ca.43)	37.8 (ca.28)	0.038	0.164	
<i>Yokosuka deep-tow</i>	main video (fixed, -81°, ***)	2/2005-	1-	DXC-990 (Sony)	CCD (1/2)	S4×5.5BMD (Fujinon)	5.5-22	16.57~61.37	12.45~48.11	0.46	2.31	

*, estimated from focal length and image sensor size

**, with wide conversion lens

***, as of April 2014 (this value may vary)

comments to improve the manuscript; the operation teams of the *Shinkai 6500* and ROV *Hyper-Dolphin* for their help in the experiments; the crews of the R/V *Natsushima* (NT13-22); and the members of Nippon Marine Enterprises, Ltd. (NME) for providing the specifications of cameras and lenses on the JAMSTEC's submersible survey platforms. This study was partially supported by the Environment Research and Technology Development Fund (S9) of the Ministry of the Environment and by the Tohoku Ecosystem-Associated Marine Sciences (TEAMS) research program of the Ministry of Education, Culture, Sports, Science and Technology (MEXT).

References

- Chevaldonné, P., and D. Jollivet (2003), Videoscopic study of deep-sea hydrothermal vent alvinellid polychaete populations: biomass estimation and behaviour, *Mar. Ecol. Prog. Ser.*, *95*, 251–262.
- Collins, P. C., B. Kennedy, J. Forde, A. Patterson, J. Copley, L. Marsh, V. Nye, R. Boschen, N. Fleming, S. -J. Ju, D. Lindsay, H. Watanabe, H. Yamamoto, J. Carlsson, and A. D. Thaler (2013), VentBase: Developing a consensus among stakeholders in the deep-sea regarding environmental impact assessment for deep-sea mining — A workshop report, *Mar. Policy*, *42*, 334–336.
- Guinan, J., A. J. Grehan, M. F. J. Dolan, and C. Brown (2009), Quantifying relationships between video observations of cold-water coral cover and seafloor features in Rockall Trough, west of Ireland, *Mar. Ecol. Prog. Ser.*, *375*, 125–138.
- Jones, D. O. B., B. J. Bett, and P. A. Tyler (2007), Megabenthic ecology of the deep Faroe-Shetland channel: a photographic study, *Deep-Sea Res. I*, *54*, 1111–1128.
- Fujikura, K., J. Hashimoto, Y. Fujiwara, and T. Okutani (1995), Community ecology of the chemosynthetic community at off Hatsushima site, Sagami Bay, Japan, *JAMSTEC J. Deep Sea Res.*, *11*, 227–241. (in Japanese with English abstract)
- Fujikura, K., J. Hashimoto, Y. Fujiwara, and T. Okutani (1996), Community ecology of the chemosynthetic community at off Hatsushima site, Sagami Bay, Japan –II: comparisons of faunal similarity, *JAMSTEC J. Deep Sea Res.*, *12*, 133–153. (in Japanese with English abstract)
- Fujikura, K., J. Hashimoto, and T. Okutani (2002), Estimated population density of megafauna in two chemosynthesis-based communities: a cold seep in Sagami Bay and a hydrothermal vent in the Okinawa Trough, *Benthos Res.*, *57*, 21–30.
- Fujikura, K., T. Okutani, and T. Maruyama (2008), Deep-Sea Life –Biological observations using research submersibles, Tokai University Press, Kanagawa, Japan. (in Japanese with English figure captions)
- Ohata, S., and L. Laubier (1987), Deep biological communities in the subduction zone of Japan from bottom photographs taken during “nautile” dives in the Kaiko project, *Earth Planet. Sci. Lett.*, *83*, 329–342.
- Seike, K., K. Shirai, and Y. Kogure (2013), Disturbance of shallow marine soft-bottom environments and megabenthos assemblages by a huge tsunami induced by the 2011 M9.0 Tohoku-Oki Earthquake, *PLoS ONE*, *8*, e65417.
- Rice, A. L., R. G. Aldred, D. S. M. Billett, and M. H. Thurston (1979) The combined use of an epibenthic sledge and a deep-sea camera to give quantitative relevance to macrobenthos samples, *Ambio. Spec. Rep.*, *6*, 59–72.
- Rice, A. L., R. G. Aldred, E. Darlington, and R. A. Wild (1982), The quantitative estimation of the deep-sea megabenthos; a new approach to an old problem, *Oceanol. Acta*, *5*, 63–72.